JOURNAL OF MATERIALS SCIENCE 30 (1995) 1338–1342

In situ reacted TiB_2–reinforced mullite

C. T. HO
Department of Mechanical Engineering, National Yun-Lin Polytechnic Institute, Yun-Lin, Taiwan, ROC

In situ formation of TiB_2 in mullite matrix through the reaction of TiO_2, boron and carbon has been studied. In hot-pressed and pressureless-sintered samples, in addition to TiB_2, TiC was also found to be dispersed phases in mullite matrix. However, in the case of pressureless-sintered samples, mullite/TiB_2 composite with 98% relative density can be obtained through a preheating step held at 1300 °C for longer than 3 h and then sintering at a temperature above 1600 °C. Hot-pressed composite containing 30 vol% TiB_2 gives a flexural strength of 427 MPa and a fracture toughness of 4.3 $MPa\,m^{1/2}$. Pressureless-sintered composite containing 20 vol% TiB_2 gives a flexural strength of 384 MPa and a fracture toughness of 3.87 $MPa\,m^{1/2}$.

1. Introduction

Mullite is an attractive material for certain structural applications because of its excellent creep resistance, low thermal expansion coefficient, better thermal shock resistance, and high temperature strength retention. However, mullite suffers from low strength and low fracture toughness. Until now, making composites by adding various toughening agents such as SiC whiskers or zirconia particles has been the most common way to toughen or strengthen mullite [1–4].

Using TiB_2 particles as a dispersed phase has been proved effective in strengthening alumina [5, 6]. Also, the high hardness ($\sim 3300\ \mathrm{kgf\,mm^{-2}}$) and good thermal conductivity ($30\ \mathrm{W\,m^{-1}\,{}^{\circ}C^{-1}}$) of TiB_2 make the Al_2O_3/TiB_2 composite an excellent cutting tool material [7]. Basically the Al_2O_3/TiB_2 composite is not difficult to densify as a pressure is applied during sintering. The problems are the high reactivity of TiB_2 with moisture, which makes direct powder mixing difficult [8], and the TiB_2 particles grow fairly fast during the sintering stage and the strengthening effect is obviously consequently reduced. Furthermore, the commercial TiB_2 powder, which is available in the particle size range 3–14 μm, is not favourable for use as a starting material [8].

If the dispersed phase can be formed *in situ* in a ceramic matrix, the particle size can be much reduced by appropriately controlling the sintering temperature and time [9, 10]. TiB_2 particles may be synthesized *in situ* through the reaction between TiN and B in a SiC matrix [11]. In the present work, we used *in situ* formation of TiB_2 in a mullite matrix through the reaction of TiO_2, boron and carbon powders, which have no handling problems in a mullite matrix by hot-pressing or pressureless sintering. It was expected that the particle size of internally synthesized TiB_2 particles would be much finer than commercial powders. In addition to identifying the TiB_2 phase, the densification, microstructure evolution and the mechanical properties of this mullite/TiB_2 composite were investigated.

2. Experimental Procedure

The starting materials used were $3Al_2O_3 \cdot 2SiO_2$ powder (average particle size 0.6 μm, purity > 99%), TiO_2 powder (average particle size 1.26 μm, purity > 99%), boron powder (average particle size 1.3 μm) and carbon powder (average particle size 0.7 μm). The starting materials were mixed in a ball mill using ethanol as solvent. The mix ratio for TiO_2, boron and carbon was designed according to the stoichiometry of TiB_2. Before sintering, the mixed powders were die-pressed at a pressure of 20 MPa to form discs of 60 mm diameter and 5 mm thickness. The discs were then placed in a graphite container and either hot-pressed at a pressure of 30 MPa, or pressureless sintered under vacuum conditions. In the case of hot-pressing (firing pattern A, as shown in Fig. 1A), the samples were preheated at 1300 °C for 4 h before hot-pressing at 1500 °C for 1 h. The pressureless-sintering profiles (firing pattern B, Fig. 1B), were preheated at 1300 °C for 0–4 h and then pressureless sintered at 1600 °C for 1 h.

The samples were examined by using X-ray diffractometer (Philips APD170 Model) and optical microscopy after being polished with diamond paste of particle size down to 1 μm. Thin foils for transmission electron microscopy (TEM) were prepared from thin slices cut using a low-speed diamond saw. These slices were then ground to a thickness of ~30–80 μm. The final thinning was carried out by ion-beam milling with a 5 kV argon-ion beam incident on both surfaces of the foil at an angle of 12°. Electron microscopy was performed using a scanning transmission electron microscope (Jeol 2000 FX).

The phase composition of the sintered samples was determined by X-ray quantitative analysis and chemical analysis. The bulk density of sintered body was determined by Archimedes' method. The flexural strength, σ_f, was measured by the four-point bending method according to the JIS 1601 standard. The fracture toughness, K_{Ic}, was measured using the

0022–2461 © *1995 Chapman & Hall*

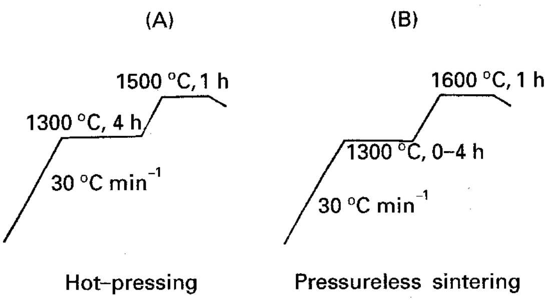

Figure 1 (A) Firing patterns for preheating at 1300 °C for 4 h and then hot-pressing at 1500 °C for 1 h. (B) Firing patterns for preheating at 1300 °C for 0–4 h and then pressureless sintering at 1600 °C for 1 h.

single-edge notched beam (SENB) method. Highly polished specimens were cut into 3 mm × 4 mm × 40 mm bars and these bars were centre-notched to one-third of their thickness using a 0.15 mm thick diamond blade. Both flexural strength and fracture toughness were measured at room temperature in a testing machine operated at a constant crosshead speed of 0.5 mm min^{-1}. Each data point was the average of at least five tests.

3. Results and discussion

3.1. Sintering and phase identification

Fig. 2a shows the X-ray diffraction (XRD) pattern of the sintered body obtained by preheating at 1300 °C for 4 h and then hot-pressed at 1500 °C in argon (firing pattern A). Besides TiB_2 and TiC, TiO_2 was retained in the mullite matrix. However, if firing pattern A was adopted (but in vacuum), while only TiB_2 and a trace amount of TiC were observed (Fig. 2b). This demonstrates that the TiO_2 phase can be eliminated by sintering in vacuum atmosphere. This indicates that an argon atmosphere is not favourable for TiB_2 formation. If the samples were pressureless sintered at 1600 °C for 1 h in vacuum (pattern B), the XRD pattern was almost the same as that of the samples sintered by pattern A (in vacuum).

From the phases identified by XRD, the chemical reaction may be described by the following equation

$$2TiO_{2(s)} + 5C_{(s)} + 2B_{(s)} \rightarrow TiB_{2(s)} + TiC_{(s)} + 4CO_{(s)} \quad (1)$$

In this reaction the standard free energy change, ΔG°, which is calculated based on JANAF thermochemical tables [12], is -287.8 kJ mol^{-1}, indicating that the reaction is possible. However, in the case of sintering in argon atmosphere, the CO gas cannot be freely released and this inhibits the previous reaction moving towards the right. Thus, the unreacted TiO_2 will remain in the mullite matrix.

3.2. Density

The density of the sintered body was measured after pressureless sintering. Fig. 3 shows the dependence of relative density on preheating time at 1300 °C for samples pressureless sintered at 1600 °C for 1 h in vacuum (pattern B). It is clearly seen that the composites containing 10 and 20 vol % TiB_2 can be densified up to 98% theoretical density after being preheated at 1300 °C for ≥ 3 h and then pressureless sintered at 1600 °C for 1 h in vacuum. This indicates that prolonging the preheating time at 1300 °C is crucial in the pumping out of the CO gas, because this gas is detrimental to densification of the composite. Densification of hot-pressed specimens in excess of 99% theoretical density (TD) was achieved.

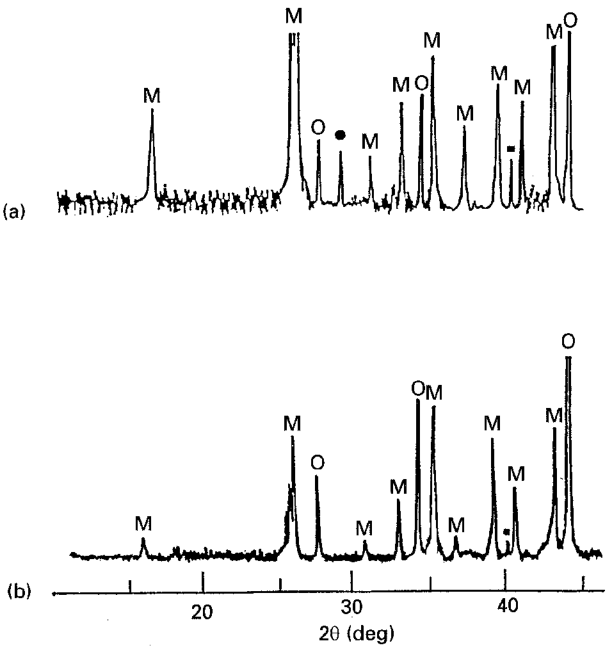

Figure 2 X-ray diffraction (XRD) patterns of the samples hot-pressed by using firing pattern A. (a) In argon, (b) in vacuum. (m) Mullite, (O) TiB_2, (■) TiC, (●) TiO_2.

On increasing the amount of synthesized TiB_2, the relative densities of the composites decrease. For instance, the composite containing 30 vol % TiB_2, after being preheated at 1300 °C for 4 h and sintered at 1600 °C for 1 h in vacuum, had a relative density of 94.5% (Fig. 3), revealing that TiB_2 particles inhibit the densification of the composites.

3.3. Microstructure investigation

Fig. 4 shows the optical micrograph of the sintered body containing 10 vol % TiB_2 which was preheated at 1300 °C for 3 h and then pressureless sintered at 1600 °C for 1 h in vacuum. The TiB_2 particles were well dispersed in the mullite matrix.

Fig. 5a shows a typical transmission electron micrograph of the composite containing 20 vol % TiB_2 obtained by preheating at 1300 °C for 4 h and hot-pressing at 1500 °C for 1 h in vacuum. It is estimated that the TiB_2 particle size ranges from 0.1–1.7 µm, much smaller than the commercially available powders, as was expected. A large number of TiB_2 particles precipitated in the intragrains of the mullite matrix, which induced the dislocation and strain contour in the surrounding matrix. The intragrain TiB_2 particles which were enclosed in mullite grains are generally round and very small. Some TiB_2 particles precipitated along the mullite grain

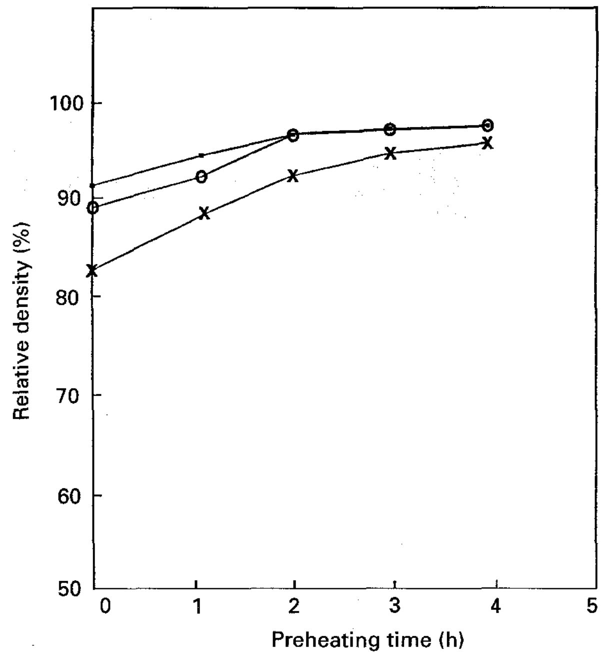

Figure 3 Relative densities of the composites as a function of preheating time at 1300 °C by pressureless sintering at 1600 °C for 1 h in vacuum (pattern B). (■) 10 vol %, (O) 20 vol %, (X) 30 vol %.

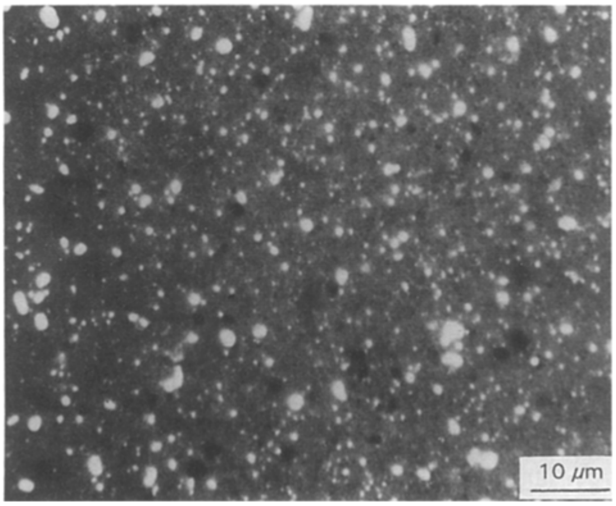

Figure 4 Optical micrograph of the composite containing 10 vol % TiB_2 obtained through preheating at 1300 °C for 3 h and then pressureless sintering at 1600 °C for 1 h in vacuum.

boundaries. The intergrain TiB_2 particles had a large mean particle size and sharp-edged grains. In the case of mullite/20 vol % TiB_2 composite, which was obtained through preheating at 1300 °C for 3 h and then pressureless sintering at 1600 °C for 1 h in vacuum, the particle size of TiB_2 and the grain size of mullite were larger than those hot-pressed at 1500 °C for 1 h, as shown in Fig. 5b.

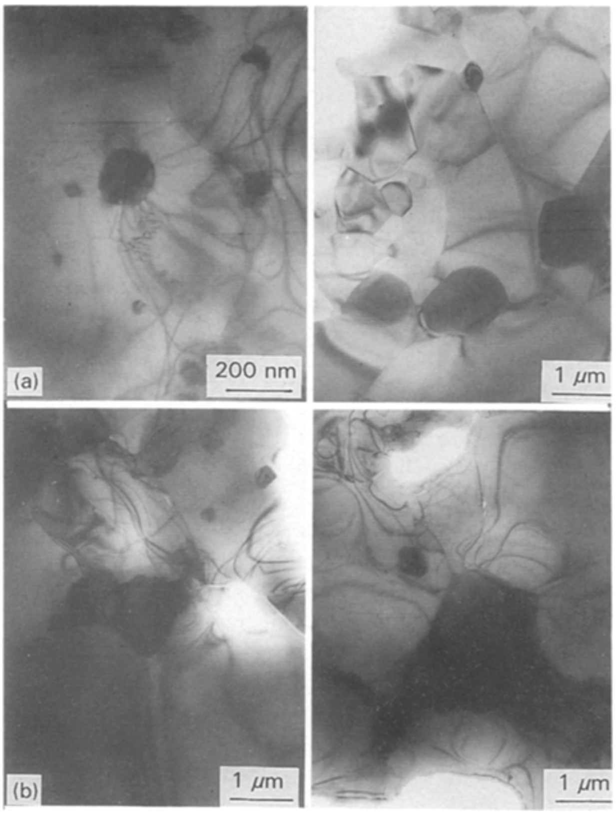

Figure 5 TEM micrograph of the composite containing 20 vol % TiB_2 obtained through (a) preheating at 1300 °C up to 4 h and then hot-pressing at 1500 °C for 1 h in vacuum, (b) preheating at 1300 °C for 3 h and then pressureless sintering at 1600 °C for 1 h vacuum.

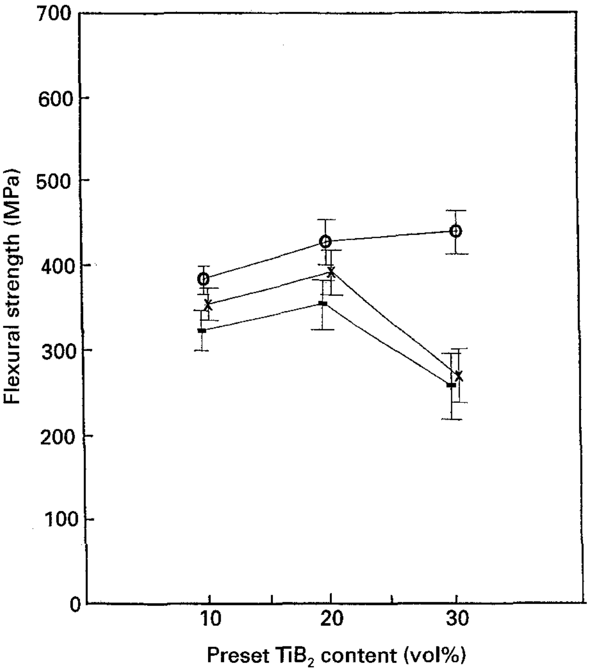

Figure 6 Dependence of flexural strength of the composites on the preset TiB_2 content. The composites were obtained through (i) preheating at 1300 °C for 4 h and then hot-pressing at 1500 °C for 1 h in vacuum (O), (ii) preheating at 1300 °C for 3 h (■) or 4 h (×) and then pressureless sintering at 1600 °C for 1 h in vacuum.

3.4. Mechanical properties

Fig. 6 shows the flexural strength of the composites through preheating at 1300 °C for 3 or 4 h and then pressureless sintering at 1600 °C for 1 h. It can be seen that the flexural strength of the composite containing 20 vol % TiB_2 was up to 384 MPa as the preheating time was above 4 h. However, in the composite containing 30 vol % TiB_2, the flexural strength decreased markedly which should be due to the low relative density as shown in Fig. 4. The flexural strength of the

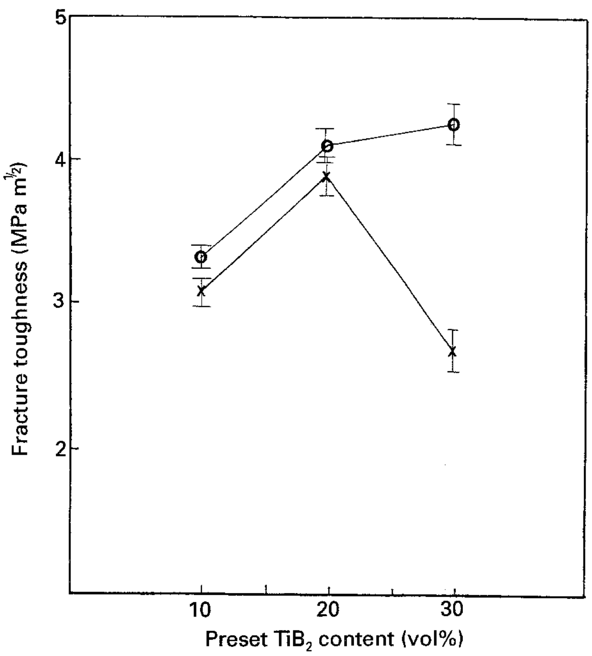

Figure 7 Fracture toughness of the composites as a function of the preset TiB_2 content. The composites were obtained through the following sintering procedures: (i) preheating at 1300 °C for 4 h and then hot-pressing at 1500 °C for 1 h in vacuum (O), (ii) preheating at 1300 °C for 4 h and then sintering at 1600 °C for 1 h in vacuum (×).

composites through preheating at 1300 °C for 4 h and then hot-pressing at 1500 °C for 1 h is also shown in Fig. 6. The flexural strength of the composite containing 30 vol % TiB_2 was up to 427 MPa.

Fig. 7 shows the fracture toughness of the composites as a function of TiB_2 content. These composites were obtained through the following sintering procedures:

(1) Preheating at 1300 °C for 4 h and then pressureless-sintering at 1600 °C for 1 h in vacuum.
(2) Preheating at 1300 °C for 4 h and then hot-pressing at 1500 °C for 1 h in vacuum.

By using sintering procedure (2), the composite containing 30 vol % TiB_2 gives a fracture toughness of 4.3 MPa $m^{1/2}$, higher than the composite containing 20 vol % TiB_2 which was sintered by using procedure (1). The error bars in Figs 6 and 7 indicate the standard deviation of measured values. The mechanical properties of the composites are superior to those of monolithic mullite. The typical strength and toughness of monolithic mullite were 200–240 MPa and 2.8 MPa $m^{1/2}$, respectively [3].

The increase of bending strength and fracture toughness, caused by incorporating dispersed TiB_2 may arise by the following reasons. It is known that TiB_2 has a higher elastic modulus (544 GPa) and thermal expansion coefficient (8.1×10^{-10} K^{-1}) than those of mullite (210 GPa, 5.3×10^{-10} K^{-1}) that can induce the compressive residual stress–strain and dislocation in the mullite matrix; this was shown in Fig. 5. Cracks can be deflected by the interaction between crack and residual stress–strain or dislocation field. The toughness of composites can be enhanced by this mechanism. The compressive residual stress in the matrix can also increase the bending strength of composites. In addition, cracks can be deflected and twisted by dispersed particles in the intergrain or intragrain of the matrix acting as fracture-resistant obstacles, which is often used to explain the higher bending strength values obtained in some composites [13].

It has been shown that the particle size of reinforcement must be larger than the critical particle size to induce microcracking toughness in the composites [14], therefore the microcracking toughening effect might be ruled our from the possible causes because of the small particle size of reinforcement in this *in situ* formed composite. The higher flexural strength and fracture toughness in the composites hot-pressed at 1500 °C for 1 h, compared with those pressureless sintered at 1600 °C for 1 h, may be due to the higher relative density (Fig. 3). Other reasons are believed to be the inhibited grain growth of mullite and the lesser coalescence of TiB_2 particles in the composites hot-pressed at 1500 °C for 1 h as discussed in Section 3.3.

4. Conclusions

In order to obtain mullite/TiB_2 composite through an *in situ* reaction between TiO_2, boron and carbon, hot-pressing and pressureless-sintering processes have been studied. The conclusions are as follows

1. In hot-pressing and pressureless sintering, in addition to TiB_2, TiC was also found to be dispersed phase in the mullite matrix.
2. The average particle size of TiB_2, obtained through the *in-situ* method, is much smaller than that of the starting powder.
3. In pressureless sintering, the mullite/TiB_2 composite can be successfully developed and densified up to 98% relative density by preheating at 1300 °C for ≥ 3 h and then sintering at 1600 °C for 1 h in vacuum.
4. The mullite/30 vol % TiB_2 composite, which shows the best performance in the mechanical test, was obtained through preheating at 1300 °C for 4 h and then hot-pressing 1500 °C for 1 h in vacuum. A flexural strength of 427 MPa and fracture toughness of 4.3 MPa $m^{1/2}$ was observed in this hot-pressed composite.
5. The composite containing 20 vol % TiB_2, preheating at 1300 °C for 4 h and then pressureless sintering at 1600 °C for 1 h in vacuum, gives a flexural strength of 384 MPa and a fracture toughness of 3.87 MPa $m^{1/2}$.

References

1. B. C. WEI and P. F. BECHER, *Am. Ceram. Soc. Bull.* **64** (1985) 298.
2. N. CLAUSSEN, *Advances in Ceramics, Vol. 12, Science and Technology of Zirconia II*, Edited by N. Claussen, M. Ruhle and A. Heuer (The American Ceramic Society, Columbus, Ohio, 1984) p. 3225.
3. N. CLAUSSEN and G. PETZOW, *J. Phys.* **47** Colloq. (Cl) (1986) Cl-693-Cl-702.

4. P. F. BECHER and T. N. TIEGS, *J. Am. Ceram. Soc.* **70** (1987) 651.
5. N. TAKAHASHI, Y. IYORI and H. HARA, *Hitachi Kinzoku Giho* **1** (1985) 41.
6. YU. I. KRYLOV, *Izv. Akad. Nauk SSSR Neorg. Mater.* **12** (1976) 1684.
7. G. V. SAMSONON and I. M. VINITSKII, "Handbook of Refractory Compounds" (IFI/Plenum, New York, 1980) p. 40.
8. H. R. BAUMGARTNER and R. A. STEIGER, *J. Am. Ceram. Soc.* **67** (1984) 207.
9. S. C. CHUANG, C. T. KUO, C. S. LEE, C. T. HO and A. K. LI, *J. Mater. Sci.* **27** (1992) 5844.
10. C. T. HO, *J. Mater. Research* **8** (1993) (in press).
11. T. TANI and S. WADA, *J. Mater. Sci.* **25** (1990) 157.
12. M. W. CHASE Jr, C. A. DAVIES, J. R. DOWNEY Jr, D. J. FRURIP, R. A. MACDONALD and A. N. SYVERUD, in "JANAF Thermochemical Tables", 3rd Edn., Part II (American Chemical Society and the American Institue of Physics for the National Bureau of Standards, New York, 1985) p. 274.
13. C. BASUDIN, F. CAMBIER, and L. DELAEY, *J. Mater. Sci.* **21** (1986) 4024.
14. A. G. EVANS and K. T. FABER, *J. Am. Ceram. Soc.* **64** (1981) 394.

Received 28 September 1993
and accepted 5 September 1994